PCCP

ROYAL SOCIETY OF CHEMISTRY

PAPER

View Article Online
View Journal | View Issue

Cite this: *Phys. Chem. Chem. Phys.*, 2021, **23**, 11907

Theoretically modelling graphene-like carbon matryoshka with strong stability and particular three-center two-electron π bonds†

Mengyang Li,‡[a] Yaoxiao Zhao,‡[a] Zhibin Gao,*[b] Kun Yuan*[c] and Xiang Zhao*[a]

Received 24th March 2021,
Accepted 29th April 2021

DOI: 10.1039/d1cp01307f

rsc.li/pccp

Carbon materials based on different hybridization of carbon atoms have drawn great attention because of their unique configurations and physical and chemical properties. Here, a previously unknown 2D carbon allotrope named L-2Gy, graphene-like carbon matryoshka graphynes (Gy) with two alkynyls (C≡C) inserted into the three-fold carbon atoms of graphene, has been constructed with considerable thermal, dynamical, and mechanical stability by using *ab initio* density functional theory. With the increasing number of alkynyls between the three-fold carbon atoms of graphene, the stability of Gy will seriously decrease. L-2Gy has a fascinating chemical bond environment consisting of sp- and sp^2-hybridized carbon atoms, and delocalized π electrons derived from the 27 three-center two-electron π bonds. This particular electronic structure plays a vital role in chemically stabilizing L-2Gy. The electronic band structure reveals the semi-metallic features of L-2Gy mainly contributed by the $p_{x/z}$ orbitals of carbon atoms. Furthermore, compared with the acknowledged catalysts for the hydrogen evolution reaction (HER), L-2Gy, as a 2D carbon allotrope, shows excellent catalytic activity for the HER.

Introduction

Carbon atoms are one of the most vital elements in life and materials science, and are capable of forming different allotropes because of their important multiform electronic configurations and various hybridizations. Graphene is one of the most famous allotropes of the carbon atom. The term "graphene" was first proposed in 1986 with pure sp^2-hybridized carbon atoms arranged in a honeycomb lattice, which has been successfully obtained with a single-atom thickness by the mechanical exfoliation of bulk graphite in 2004.[1] After that, graphene was characterized on a variety of substrates with unique physical and chemical properties,[2] such as a strong ambipolar electric field effect, high carrier mobility, and a quantum Hall effect, in experiments.

On the other hand, graphene-derived materials, including graphene oxide, fluorographene, graphane, and graphynes (Gy), have been obtained by the introduction of functional groups in graphene since its first successful isolation. Specifically, graphene oxide, the synthesis of which was first demonstrated in 1895, is a kind of special derivative of graphene, and now is the substrate to obtain graphene.[3] Compared with the pristine graphene, the mechanical strength of graphene oxide is a little lower, but enough for fabricating composite materials.[4] Furthermore, the electronic and optical properties of graphene oxide can be selectively controlled *via* the removal or addition of oxygen-containing groups, which determines the semiconducting or insulating nature of graphene oxide, leading to promising applications in electric and optical devices, spintronic devices, chemical or biological sensors, and electrode materials.[5] Fluorinated graphene, named fluorographene, is another important derivative of graphene. The structure and chemical compositions of fluorographene represented by CF and C_2F are well understood, and fluorographene has definite applications as the anode material of primary lithium batteries and super-hydrophobic materials.[6] A thoroughly hydrogenated derivative of graphene, named graphane the chemical composition of which is CH, has been initially predicted by first-principles calculations[7] and synthesized in 2009.[8] Graphane, consisting of sp^3 C–C bonds, has two conformations, chair and boat types, which could be

[a] *Institute of Molecular Science & Applied Chemistry, School of Chemistry, State Key Laboratory of Electrical Insulation and Power Equipment & MOE Key Laboratory for Nonequilibrium Synthesis and Modulation of Condensed Matter, Xi'an Jiaotong University, Xi'an 710049, China. E-mail: xzhao@mail.xjtu.edu.cn*
[b] *State Key Laboratory for Mechanical Behavior of Materials, Xi'an Jiaotong University, Xi'an 710049, China. E-mail: zhibin.gao@xjtu.edu.cn*
[c] *College of Chemical Engineering and Technology, Tianshui Normal University, Tianshui, 741001, China. E-mail: yuankun@tsnu.edu.cn*

† Electronic supplementary information (ESI) available: Optimal conformations; stiffness tensor matrixes; crystal structures and localized orbital locator (LOL) maps; molecular AdNDP orbitals; band structure on HSE06; possible absorbed configurations; calculation details, and fractional coordinates for L-2Gy and L-3Gy. See DOI: 10.1039/d1cp01307f

‡ These authors contributed equally to this work.

considered as two-dimensional analogs of diamond: the chair type to the cubic diamond and the boat type to the hexagonal one.[9] Furthermore, hydrogenation could highly transform conductive zero-overlap semi-metallic graphene into the insulating one, and the band gap of hydrogenated graphene, the same as in graphene oxide, also depends on the degree of hydrogenation.[10]

Recently, the construction of carbon materials with different hybridization states of the carbon atom attracts tremendous interest because the different hybridization states of the carbon atom always mean the distinguished properties of new carbon materials. For example, the sp^3-hybridized carbon atoms endow diamond with excellent mechanical properties.[11] The lattic structure of sp^2- + sp^3-hybridized, sp- + sp^3-hybridized, and sp- + sp^2- + sp^3-hybridized carbon atoms. The most famous one is Gy which is composed of sp + sp^2-hybridized carbon atoms, showing a perfect planar conformation. The lattice structure of renowned Gy, successfully constructed and prepared on copper substrates *via* a cross-coupling reaction with hexaethynylbenzene in 2010 by Li's group,[12] can be simply viewed as a consequence of replacing a portion of sp^2-hybridization C–C bonds in graphene by carbynes. The various arrangements of carbynes will lead to different conformations. The insertion of one carbyne into each bond of graphene yields the most graphene-like 2D carbon-matryoshka materials, called α-graphynes (α-Gy or here L-1Gy), which share the hexagonal Bravais lattice with graphene.[13] In L-1Gy, the threefold carbon atoms are connected by one carbyne. Clearly, a linear chain with carbynes, connecting the threefold honeycomb sites, in different numbers is conceivable. Gy would exhibit remarkable mechanical, electrical, and chemical properties due to the presence of carbynes. The electronic properties and lattice stability are the crucial steps in determining the promising applications of Gy. Then, some interesting questions arise, whether there is a critical point for the number of carbynes between the threefold honeycomb sites in Gy determining their stabilities and what is the role of carbynes for Gy in their physical and chemical features.

Herein, the stability of Gy containing carbynes, between the threefold honeycomb sites, in different numbers was investigated by the state-of-the-art first principles calculations. The results reveal that L-2Gy (Fig. 2), in which two carbynes connect the threefold honeycomb sites, is another thermodynamically, mechanically, and dynamically stable Gy. Although L-Gy and well-known graphyne, as the allotropes of carbon atoms, contain sp- and sp^2-hybridized carbon atoms, their geometries are distinguished from each other. The research on stability reveals that the structure (L-*n*Gy, n = 1, 2, and 3) would become unstable when the number of carbynes (n) connecting the threefold honeycomb sites in Gy is more than two. Then, the electronic structures and mechanical features of L-2Gy were thoroughly studied. Furthermore, because of the good flexibility of L-2Gy and the various adsorbed sites in L-2Gy for hydrogen atoms, we have tried to explore the catalytic activity of L-2Gy for the hydrogen evolution reaction (HER). Compared with some acknowledged good catalysts for the HER, L-2Gy shows excellent catalytic activity for the HER.

Calculation methods

All of the first-principles calculations were carried out based on Kohn–Sham density functional theory (DFT) with the Vienna *ab initio* simulation package (VASP).[14] The generalized gradient approximation as parameterized by Perdew, Burke, and Ernzerhof (PBE) for the exchange–correlation functional[15] and a gamma-centered k-point sample mesh of $7 \times 7 \times 1$ were used to relax the geometries. A plane-wave basis set with a kinetic energy cutoff of 400 eV is used to expand the valence electron wave function. The convergence criteria of the energy in electronic SCF iterations and the force in ionic step iterations are 1.0×10^{-8} and 5.0×10^{-2} eV, respectively. A vacuum slab of at least 20 Å was used in order to eliminate the interactions between the layers of Gy. The phonon dispersions were calculated on the basis of a $2 \times 2 \times 1$ supercell for Gy by using density functional perturbation theory (DFPT) as implemented in the Phonopy code.[16] For the electronic structure calculation of L-2Gy, the reciprocal space is sampled with a k-grid density of $30 \times 30 \times 1$ under the consideration of accuracy and efficiency. Furthermore, the hybrid functional of Heyd, Scuseria, and Ernzerhof (HSE06) was carried out to ensure the accurate band gap of L-2Gy based on the PBE, because the previous report indicates that the PBE functional usually underestimates the band gap of semiconductors and insulators.[17] The mechanical properties of L-2Gy, such as elastic constants, Young's modulus, and Poisson's ratio, are calculated based on the stiffness matrix and with the help of the VASPKIT package.[18]

Additionally, the optimal conformations of C_nH_2 ($2 \leq n \leq 8$) were determined and all of them are free from the imaginary frequency on the B3LYP/6-311G(d,p).[19] In order to further expose the hybridization states of carbon atoms and the nature of bonds in L-2Gy, the natural bond orbital (NBO) calculations were carried out for the simplified model of L-2Gy on the B3LYP/6-311G(d,p), and the dangling atoms in this model (Fig. 4a) were saturated with hydrogen atoms. In graphene, three 6c-2e π bonds of benzene are determined to elucidate the electronic configuration and delocalization of graphene.[20] Adaptive natural density partitioning (AdNDP) is a powerful method to elucidate the multicenter (nc-2e) bonds.[21] Thus, the nc-2e bonds in $C_{30}H_6$ were searched to clearly show the nature of bonds in L-2Gy by the AdNDP method implemented in the Multiwfn software.[22] All of the above-mentioned density functional theory calculations were conducted with the Gaussian 16 program.[23]

Results and discussion

Stability

In order to clarify the stability of Gy with carbynes, connecting the threefold honeycomb carbon atoms, in different numbers, the optimal configurations of C_nH_4 ($2 \leq n \leq 8$) were determined. When n is an even number, C_nH_4 (n = 2, 4, 6, and 8) possesses planar configurations (Fig. S1, ESI†), meaning that Gy with even numbers of twofold carbon atoms along the chains would be the potential stable structures for extended 2D materials, like

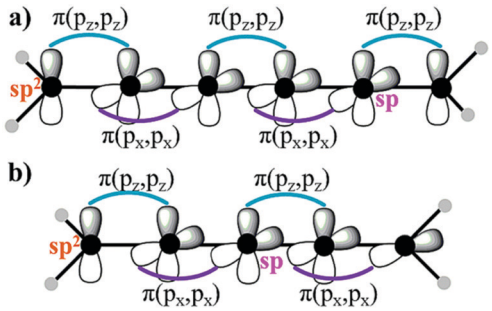

Fig. 1 (a) C_6H_4 with coplanar methylene (CH_2) at the edges; (b) C_5H_4 with perpendicular methylene (CH_2) at the edges; including their π-bonding scheme along the chains.

graphene.[1,13] The NBO results reveal exclusively olefinic bonds in the carbon skeleton of C_nH_4 (n = 2, 4, 6, and 8) known as cumulenes, consisting of sp^2-hybridized threefold carbon atoms and sp-hybridized twofold carbon atoms. In addition, the minimum frequencies of C_nH_4 (n = 2, 4, 6, and 8) decrease with the increasing number of carbon atoms, suggesting that C_8H_4 is located at the potential energy surface with a shallow potential well and relatively low stability compared with that of C_nH_4 (n = 2, 4, and 6). On the other hand, C_nH_4 (n = 3, 5, and 7) preferred an extended tetrahedral conformation in which the methylene groups at the two terminations of the molecules are perpendicular to each other.[24] In a previous report, the authors explain the reason why C_3H_4 and C_4H_4 preferred extended tetrahedral and planar conformations, respectively, according to the hybridization orbitals of carbon atoms, also as shown in Fig. 1 for C_6H_4 and C_5H_4.[13] Thus, Gy with one (αGy or L-1Gy), two (L-2Gy), and three (L-3Gy) carbynes connecting the threefold sp^2-hybridized carbon atoms are potential chemically stable 2D graphene-like materials, like carbon matryoshka, with a hexagonal structure the same as those of the prominent graphene and hexagonal boron nitride.[1,25]

A previous report has clarified well the stability of αGy (L-1Gy) whose lattices are the extended analogues of butatriene.[13] Similarly, the lattices of L-2Gy and L-3Gy are the extended analogues of C_6H_4 and C_8H_4 (Fig. S1, ESI†), respectively. The structural optimizations of L-2Gy and L-3Gy were performed with *ab initio* DFT calculations, and their optimal structures are shown in Fig. 2. The lattice constants are $|\vec{a}| = |\vec{b}| = 11.4225$ Å for L-2Gy and $|\vec{a}| = |\vec{b}| = 15.8189$ Å for L-3Gy, and both of them belong to *P*6/*mmm* (space group no. 191), which is just like that of the graphene.[1] There are 14 and 20 independent atoms for L-2Gy and L-3Gy, respectively, based on the group Wyckoff positions, whose optimized fractional coordinates are given in the ESI.† As shown in Fig. 2, the bond lengths are 1.39, 1.24, and 1.33 Å for C1–C2, C2–C3, and C3–C4 bonds in L-2Gy, respectively, and 1.39, 1.24, 1.32, and 1.24 Å for C1–C2, C2–C3, C3–C4, and C4–C5 bonds in L-3Gy, respectively. All of these bond lengths in L-2Gy and L-3Gy are similar to the annulene with a unique bond length close to the double bonds in C_6H_4 and C_8H_4 (Fig. S1, ESI†), respectively. The distance between C1 and C5 (C6) in L-2Gy is 11.42 (13.19) Å, and that between C1

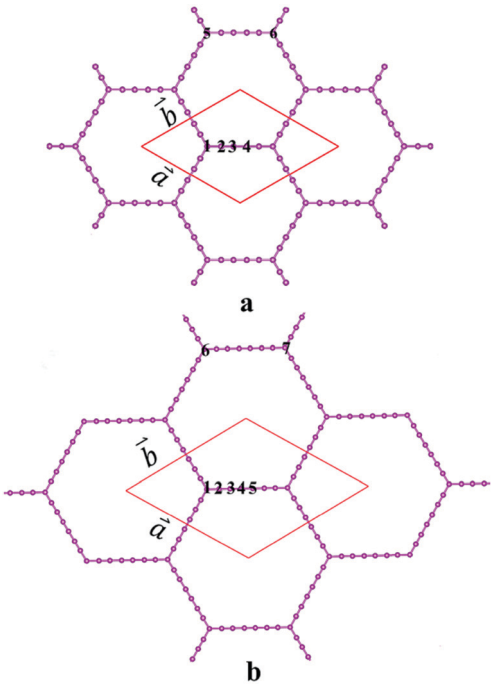

Fig. 2 Geometries of (a) L-2Gy and (b) L-3Gy. All of the atoms are carbon.

and C6 (C7) is 15.82 (18.27) Å in L-3Gy, which gives the evidence for the size of their porous hexagonal structures. In addition, a much larger porous structure generally means much larger flexibility, and thus we speculate that L-3Gy possesses higher flexibility than L-2Gy, which will be reflected in the lattice dynamic stability and confirmed by the mechanical study.

The phase stability of different Gy, including L-2Gy and L-3Gy, was evaluated by their formation energy. If the formation energy of a structure is negative, it will be considered to be thermodynamically stable with respect to decomposition into elements. The formation energy of Gy (C_n) per carbon atom is defined as[26]

$$\Delta E(C_n) = (E(C_n) - n\mu_C)/n$$

where $\Delta E(C_n)$ is the formation energy per carbon atom for Gy; $E(C_n)$ is the total energy of Gy calculated by *ab initio* DFT; and the chemical potential (μ_C) of the C atom is the cohesive energy of the graphene (−7.906 eV).[27] Here, the calculated formation energies are −0.35 eV per atom and −0.34 eV per atom for L-2Gy (C_{14}) and L-3Gy (C_{20}), respectively, showing their thermal stability. Furthermore, the more negative formation energy of L-2Gy than that of L-3Gy indicates the much more thermal stability of L-2Gy compared with L-3Gy despite the 0.01 eV difference in their formation energies.

To further explore the lattice dynamic stabilities of L-2Gy and L-3Gy, their phonon band structures were calculated by using DFPT as implemented in the Phonopy code.[16] As shown in Fig. 3, the absence of an imaginary mode in the whole 2D reciprocal space for L-2Gy manifests its lattice dynamical stability. However, L-3Gy possesses large imaginary frequencies even in the whole reciprocal space. The poor lattice dynamic stability of L-3Gy is due to the large flexibility, which is verified

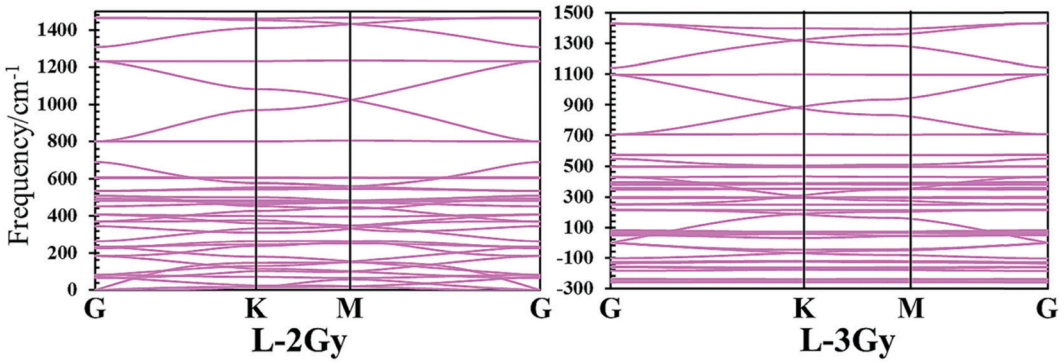

Fig. 3 Phonon band structures for L-2Gy and L-3Gy based on a 2 × 2 × 1 supercell.

by the vibrational mode of its phonon band with the most negative band. Compared with the graphene, L-1Gy, and L-2Gy, the inner diameter of the hexagon in L-3Gy becomes much larger leading to much higher flexibility. This would be revealed by the mechanical features of L-2Gy and L-3Gy shown below. Then, *ab initio* molecular dynamics simulation was performed for thermally stable L-2Gy to determine its dynamic stability using a canonical ensemble and Nosé–Hoover thermostat at 1000 K for 10 ps. A video named MD.avi as shown in the ESI† indicated that the robustness and structure of our proposed L-2Gy do not suffer significant distortion or transformation after heating at 1000 K for 10 ps with a time step of 2 fs.

On the other hand, previous reports indicate that mechanical stability should be considered for a valuable 2D material.[17a,20,28] Generally, for any mechanically stable 2D material, a necessary requirement, but not a sufficient condition, must be satisfied, that is, $C_{11}C_{22} - C_{12}^2 > 0$ and $C_{66} > 0$.[17a,20,29] The stiffness matrixes of L-2Gy and L-3Gy are shown in Table S1 (ESI†). Here, the calculated four elastic stiffness constants of L-2Gy are $C_{11} = C_{22} = 25.029$ GPa, $C_{12} = 23.359$ GPa, and $C_{66} = 0.523$ GPa, and those of L-3Gy are $C_{11} = C_{22} = 18.615$ GPa, $C_{12} = 18.209$ GPa, and $C_{66} = 0.331$ GPa. Obviously, the results of $C_{11}C_{22} - C_{12}^2 > 0$ with a positive C_{66} verified the mechanical stabilities of L-2Gy and L-3Gy. As shown in Table S1 (ESI†), it can be seen that all of the six eigenvalues are positive for L-2Gy and L-3Gy, further confirming their mechanical stability. However, compared to the eigenvalues of the stiffness constants of L-2Gy with those of L-3Gy, the mechanical stability of L-2Gy is higher than that of L-3Gy intuitively derived from the larger flexibility of L-3Gy than that of L-2Gy, which will be confirmed below by their mechanical study. Although L-2Gy and L-3Gy are chemically, thermally, and mechanically stable, only L-2Gy shows good lattice dynamical stability in combination with much better mechanical and thermal stability. Thus, L-2Gy was here predicted as another stable graphene-like Gy following previously proposed αGy (L-1Gy).[13] Although there is no experimental information on L-2Gy proposed in the present work, several reasonable experimental methods,[30] including chemical vapor deposition (CVD),[30a] close-spaced vapor transport (CVT),[30b] flux growth,[30c] a high pressure flux method,[30d] and epitaxial growth,[30e] have been successfully proposed to synthesize 2D graphene and graphene-like materials in general. Actually, L-2Gy, as a graphene-like material, shows considerable dynamical, mechanical, and thermal stability. Accordingly, there is sufficient justification to believe that all of these general experimental methods to yield graphene would be the promising candidate methods in the experiment to synthesize L-2Gy theoretically proposed here. Furthermore, an impartial speculation, that Gy would be unstable if the number of carbynes connecting the threefold carbon atoms is more than two, was proposed to give the guidance on synthetic chemistry in the future.

Bonding analysis and electronic structures of L-2Gy

For further exploring the chemical bond quantitatively, a super model for L-2Gy (Fig. 4a) was built, in which marginal threefold atoms were saturated by hydrogen atoms. Considering the negligible fringe effect, we just focus on the primitive cell in the center region of the super model of L-2Gy, which is marked by a red box. The same calculations were also carried out for the graphene and L-1Gy (Fig. S2, ESI†) with delocalized π electrons. Recently, a similar method has been successfully applied for investigating the electronic structures of the novel two-dimensional borophene, super-B.[20] As shown in Fig. 4a, except for the threefold carbon atoms, two of them, as examples, marked by a blue circle, possess a sp^2-hybridized state, and all of the other carbon atoms possess a sp-hybridized state based on the NBO analysis. Notably, there are no typical single and triple bonds between the carbon atoms, and the lengths of the bonds in L-2Gy, C1–C2 (1.39 Å), C2–C3 (1.24 Å), and C3–C4 (1.33 Å), shown in Fig. 2, tend to average. This phenomenon is similar to that of annulene (C_6H_4). These bond lengths are longer than the normal triple bonds and shorter than the normal double bonds leading to large delocalized electrons on the plane network of L-2Gy. This bonding feature in L-2Gy also occurs in L-1Gy.[13] In order to confirm the degree of delocalized electrons on L-2Gy, the localized orbital locator (LOL) maps are plotted for L-2Gy as shown in Fig. 4b, and also for graphene and L-1Gy (Fig. S2, ESI†) as the references. Compared with the graphene and L-1Gy, it is clear that the π electrons of the sp- and sp^2-carbon atoms are delocalized on the whole plane network of L-2Gy. All of these delocalized π bonds, analogous with graphene and L-1Gy, significantly contribute to the stability of L-2Gy. The novel allotrope of boron, named super-B, was proposed based on *ab initio* first-principles

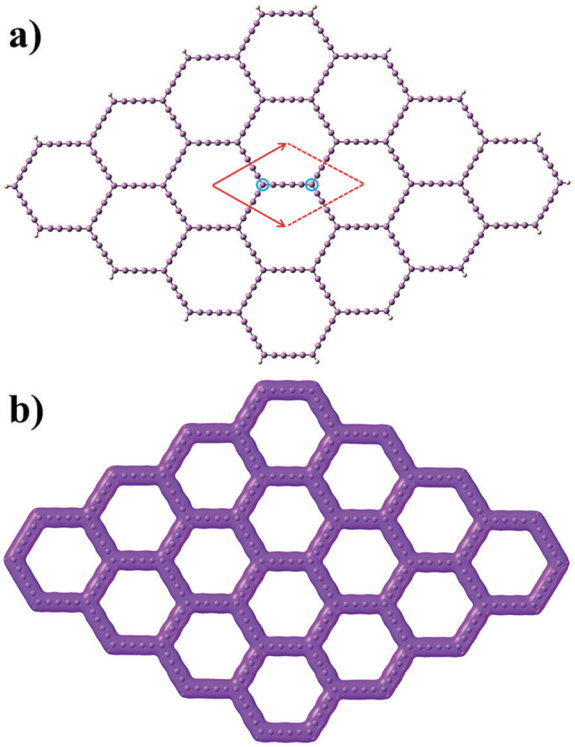

Fig. 4 Crystal structures of (a) L-2Gy. The marginal threefold carbon atoms are saturated by hydrogen atoms and its primitive cell is marked by a red box. Localized orbital locator (LOL) map (b) for L-2Gy with an isovalue of 0.05.

calculations, and the nature of its stability is also derived from the delocalized π electrons.[20] As seen from Fig. 4 and Fig. S2 (ESI†), the delocalization of π electrons slightly decreased with the increasing diameter of the hexagon in graphene, L-1Gy, and L-2Gy.

As is known to all, the large delocalization of π electrons on graphene is derived from the three delocalized 6c-2e π bonds of the benzene unit.[20,31] The relationship between benzene and graphene is the same as that between hydrogenated L-2Gy ($C_{30}H_6$) and L-2Gy, as well as that between hydrogenated L-1Gy ($C_{18}H_6$) and L-1Gy. The molecular orbitals of benzene based on the AdNDP are shown in Fig. S3 (ESI†) including 12 2c-2e σ bonds and three delocalized 6c-2e π bonds in accord with previous reports.[20,31] L-1Gy has been proposed as the first graphene-like Gy,[13] and the nature of the bonds in L-1Gy was also explored here to be compared with graphene and L-2Gy. The AdNDP molecular orbitals of $C_{18}H_6$ (L-1Gy) are shown in Fig. S4 (ESI†), and there are 24 2c-2e σ bonds, six localized 2c-2e π bonds, and nine delocalized 3c-2e π bonds. For these AdNDP orbitals of $C_{18}H_6$ (L-1Gy), six localized 2c-2e π bonds comprising p_x orbitals, parallel to the plane of the molecule ($C_{18}H_6$), of sp-hybridized carbon atoms, and nine delocalized 3c-2e π bonds are built with the p_z orbitals, perpendicular to the plane of the molecule ($C_{18}H_6$), of all sp- and sp^2-hybridized carbon atoms. All of these *n*c-2e π orbitals form a large delocalized π orbital shown in Fig. S2 (ESI†). Based on the above discussion on the stability of L-2Gy governed by the delocalized π electrons, the 36 localized 2c-2e σ bonds are shown in Fig. S5 (ESI†) for hydrogenated L-2Gy ($C_{30}H_6$) and 27 delocalized 3c-2e π bonds are shown in Fig. 5, which is also in accord with the nature of annulene based on the NBO analysis in Fig. 4a. There are 12 3c-2e π bonds for $C_{30}H_6$ parallel to the plane of the molecule, which comprised the p orbitals of all carbon atoms in $C_{30}H_6$. Additionally, 15 3c-2e π bonds perpendicular to the plane of $C_{30}H_6$ comprised the p orbitals from the sp-hybridized carbon atoms in $C_{30}H_6$. All of these delocalized 3c-2e bonds of $C_{30}H_6$ are the essential reasons for the delocalized π electrons on the whole plane of L-2Gy. Besides, no Jahn–Teller distortion was found for L-2Gy by optimizing the atomic position in a large supercell.

The electronic band structure and projected density of states (PDOS) of L-2Gy are shown in Fig. 6. It can be seen that only two bands in the reciprocal space cross at the *M* point. A previous report reveals that both local density approximation (LDA) and PBE approaches usually underestimate the band gap of semiconductors and insulators.[17a,32] Thus, a hybrid functional of HSE06 was determined for a more accurate calculation on the band structure of L-2Gy (Fig. S6, ESI†). The band structure of L-2Gy (Fig. S6, ESI†) based on HSE06 is similar to that based on PBE, confirming the exact result of the electronic structure of L-2Gy at the PBE level. Then, we believe that the intrinsic L-2Gy is a semi-metal, like graphene.[5a,9,32c,33] The carrier mobility, including holes and electrons, was evaluated for graphene and L-2Gy based on the deformation potential theory, because of the interesting band structure of L-2Gy. Graphene and L-2Gy are allotropes of the carbon atom. Under the same environmental conditions, their carrier mobility is inversely proportional to their effective masses, m_e^* for electrons and m_h^* for holes. The effective masses of electrons m_e^* along $G \rightarrow M$ are $0.643m_0$ and $0.118m_0$ for graphene and L-2Gy, respectively, meaning that the electron mobility of L-2Gy is five times higher than that of graphene. Additionally, the effective masses of holes m_h^* along $G \rightarrow M$ are $1.029m_0$ and $0.042m_0$ for graphene and L-2Gy, respectively, meaning that the hole mobility of L-2Gy is 24 times higher than that of graphene. Clearly, the carrier mobility of L-2Gy is higher than that of graphene because of the interesting electronic structures of L-2Gy (Fig. 6).

The results of PDOS indicate that the electronic structures of L-2Gy are entirely dominated by the p orbitals, especially the p_x and p_z orbitals. Furthermore, according to the AdNDP molecular orbitals for L-2Gy, the delocalized π bonds parallel to the plane of the molecule are formed by the p_x orbitals of sp-hybridized carbon atoms and the delocalized π bonds perpendicular to the plane of the molecule are formed by the p_z orbitals of sp- and sp^2-hybridized carbon atoms. Thus, the unpaired p_x electrons of sp-hybridized carbon atoms on each atomic site join to form a delocalized collective π system parallel to the plane of the molecule, and the unpaired p_z electrons of all carbon atoms on each atomic site join to form a delocalized collective π system perpendicular to the plane of the molecule, turning the material into a semi-metal. Notably, in graphene, there are only sp^2-hybridized carbon atoms, and its delocalized π bond is only contributed by the p_z orbitals.[32c,33a] Notably, like in graphene,

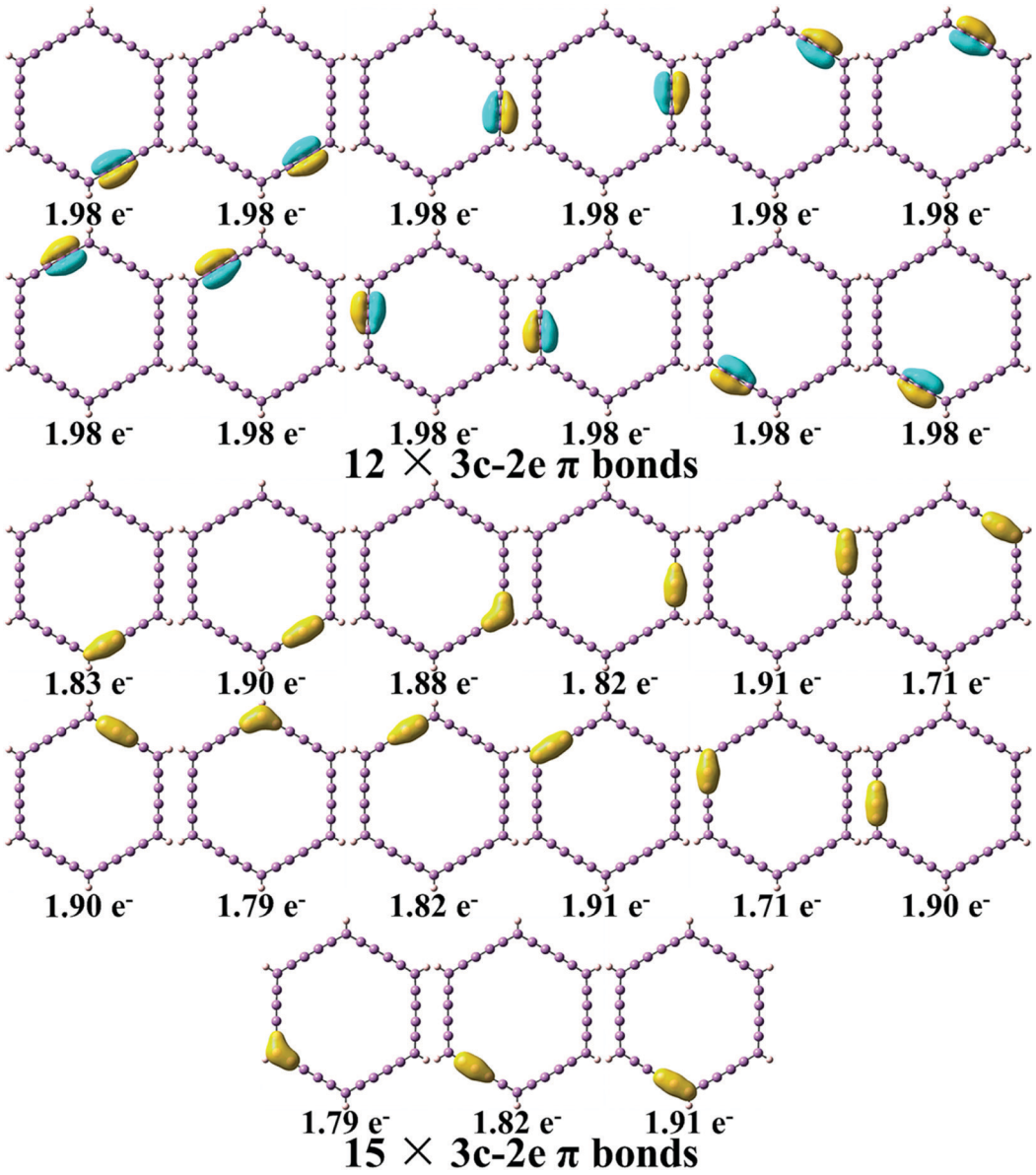

Fig. 5 Molecular orbitals for the optimized $C_{30}H_6$ based on the AdNDP method, including the occupations of electrons and types of bonds.

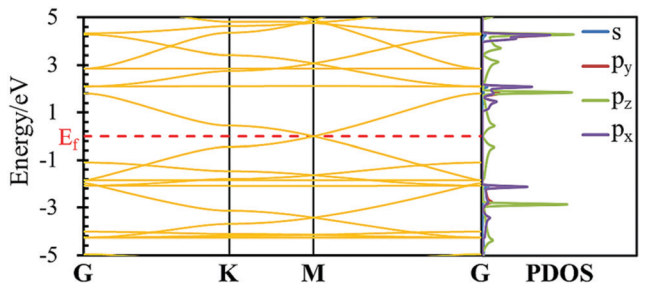

Fig. 6 Electronic band structure and projected density of states (PDOS) based on the PBE level for L-2Gy.

the electronic behaviors around the Fermi level of L-2Gy are entirely dominated by the p_z orbital of the carbon atoms.

Mechanical features

Based on the phonon band structure, there are several imaginary frequencies for L-3Gy indicating its instability. Considering the size of the hexagon hole in graphene, L-1Gy, L-2Gy, and L-3Gy, we speculate that the instability of L-3Gy is due to its large flexibility with the largest hexagon. In order to clearly explore this question, the mechanical data, shown in Table 1, reflecting their flexibility, were calculated using the Voigt–Reuss–Hill approximation[18,34] based on the stiffness tensor matrixes in Table S1 (ESI†) for L-2Gy and L-3Gy and in Table S2 (ESI†) for graphene and L-1Gy. Clearly, the values of the bulk modulus (K), shear modulus (G), and Young's modulus (E) would decrease with the increasing number of carbynes connecting threefold carbon atoms in graphene, L-1Gy, L-2Gy, and L-3Gy, indicating the enhancement of their flexibility. L-3Gy has the largest

Table 1 Mechanical features, including bulk modulus (K) in GPa, shear modulus (G) in GPa, Young's modulus (E) in GPa, isotropic Poisson's ratio (ν), and Debye temperature (Θ) in K, for graphene, L-1Gy, L-2Gy, and L-3Gy

Materials	K/GPa	G/GPa	E/GPa	ν	Θ/K
Graphene	21.95	16.45	39.48	0.20	599.67
L-1Gy	9.74	2.63	7.23	0.38	274.68
L-2Gy	6.32	1.45	4.05	0.39	220.02
L-3Gy	4.79	0.88	2.50	0.41	180.70

flexibility with the smallest values of K (4.79 GPa), G (0.88 GPa), and E (2.50 GPa). On the other hand, Poisson's ratio (ν) is a fundamental mechanical property of materials, which reflects the transverse strain response to the applied uniaxial load.[35] A large ν means that the material is much easier and more flexible to be deformed even under small stress. Clearly, L-3Gy possesses the largest ν of 0.41 again confirming its much larger flexibility. The flexibility of Gy would be much more prominent with the increasing number of carbynes connecting the threefold carbon atoms in graphene. Here, the reason why Gy is unstable when the number of carbynes connecting the threefold carbon atoms is more than two in graphene is clearly derived from the flexibility of its structures. The instability of L-3Gy is also in accord with the relatively low stability of C_8H_4, whose lowest frequency is also the lowest one compared with that of C_2H_4, C_4H_4, and C_6H_4 with planar geometries.

Compared with the electronic structure of graphene, the stability of L-2Gy is attributed to the large delocalized π electrons as in the case of graphene. The Debye temperature (Θ) can be used to accurately estimate the mean sound velocity, which arises from the atomic vibrations in theory involving phonons.[36] Graphene has the largest Θ of about 600.0 K because of the strongest interactions between the atoms. In contrast, L-3Gy has the smallest Debye temperature (Θ = 180.70 K) suggesting much weaker interactions between the atoms. As for diamond with the largest hardness among the allotropes of the carbon atom, its Θ is around 1880 K.[37] Furthermore, because of the low mass of lead and the weak interactions between the lead atoms, the Θ of lead in crystals is not more than 100 K.[38] The change in Θ of graphene, L-1Gy, L-2Gy, and L-3Gy is the same as the changing tendency of their elastic moduli.

Hydrogen evolution reaction

The catalytic performance of L-2Gy for the hydrogen evolution reaction (HER) was explored. As shown in Fig. 4a and Fig. S7 (ESI†), we considered all of the possible configurations with the absorption of the H atom on L-2Gy, and the most favorable configuration of the absorbed H atom is 2, in which the H atom is absorbed on top of the sp-hybridized C2 atom as shown in Fig. 2a, with the lowest relative energy. The calculated adsorption energies (E_{ads}) shown in Table 2 for the possible configurations with the absorption of the H atom on L-2Gy are 0.67, 0.11, 0.23, 1.87, 0.40, and 1.12 eV, respectively, for 1, 2, 3, 4, 5, and 6 in Fig. S7 (ESI†). Clearly, the results on E_{ads} also support that the configuration of 2 is the most favorable one for the absorbed H atom in accord with the results based on their relative energies. In addition, the bond length between the absorbed hydrogen atom and the corresponding carbon atom is 1.10 Å, which is the same as the general bond length (1.10 Å) of the C–H bonds in benzene, indicating the strong ability of the absorbed H atom for L-2Gy. On the other hand, the excellent catalytic performance for the HER not only depends on the ability to absorb the H atom, but is also related to the ability to release the H atom. Notably, a previous report reveals that the value of active Gibbs free energy (ΔG_H) should be nearly close to zero for an ideal catalyst for the HER.[39] The calculation details of ΔG_H for the HER are given in the ESI.† As shown in Fig. 7 and Table 2, the calculated ΔG_H for the configuration of 2 is 0.12 eV which is smaller than the ΔG_H for the HER catalysts based on the configurations of 1 (0.88 eV), 3 (0.38 eV), 4 (1.87 eV), 5 (0.55 eV), and 6 (1.24 eV). This value (ΔG_H = 0.12 eV) can be comparable to those of the previously reported other good catalysts for the HER, such as P-InP_3 (ΔG_H = 0.10 eV),[39a] Pt (ΔG_H = −0.16 eV),[39b] 1T′-MoS_2 (ΔG_H = 0.13 eV),[39c] Mo_2S_6 nanowires (ΔG_H = −0.05 eV),[39d] the 2H-1T hybrid phase of MoS_2 monolayers (ΔG_H = −0.13 eV),[39e] and 1T-WS_2 nanosheets under strain (ΔG_H = 0.09–0.49 eV),[39f] indicating that L-2Gy exhibits high catalytic activity for the HER. Although graphene-based materials, including doped graphene structures and oxidized graphene, have presented good catalysis for the HER,[39g,h] pristine graphene has not shown clearly its potential ability as an electrode material towards the HER up to now.[40] The graphene-like structure L-2Gy would be the potential allotrope of the carbon atom showing promising catalytic activity for the HER. In comparison with the graphene derivatives doped with other atoms, L-2Gy for the HER catalysis will hardly produce impurities, except for H_2.

Table 2 Absorption energies E_{ads} (eV), Gibbs free energy ΔG_H (eV), and bond length d (Å) between the hydrogen atom and the absorbed carbon atom

Configurations	E_{ads}/eV	ΔG_H/eV	d/Å
1	0.67	0.88	1.12
2	0.11	0.12	1.10
3	0.23	0.38	1.11
4	1.87	1.87	1.85
5	0.40	0.55	1.10
6	1.12	1.24	1.11

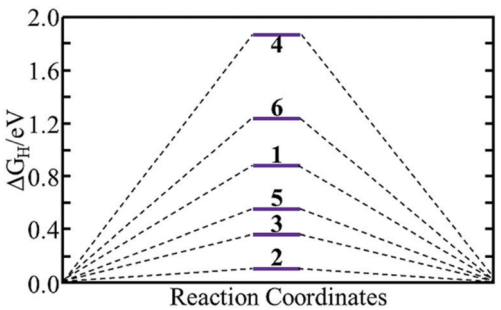

Fig. 7 Gibbs free energy ΔG_H following the reaction coordinates.

Conclusions

In summary, a previously unknown allotrope of the carbon atom, L-2Gy, with considerable thermal, dynamical, and mechanical stability has been proposed and constructed based on graphene and alkynyls. We have revealed the relationship between the number of alkynyls inserted into the three-fold carbon atoms of graphene and the stability of graphene derivative Gy. With the increasing number of alkynyls between the three-fold carbon atoms of graphene, the stability of Gy will seriously decrease, accompanied by increasing flexibility. While the number of alkynyls between the three-fold carbon atoms of graphene is less than three, Gy and graphene show excellent stability. Conversely, Gy would exhibit enhanced flexibility and awful stability. L-2Gy as a novel allotrope of the carbon atom has a fascinating chemical bond environment consisting of sp- and sp^2-hybridized carbon atoms, and delocalized π bonds, like graphene, derived from the 27 × 3c-2e π bonds based on NBO and AdNDP analysis. This particular electronic structure plays a crucial role in chemically stabilizing L-2Gy. Furthermore, compared with the acknowledged catalysts for the HER, 2D-carbon allotrope L-2Gy shows catalytic activity for the HER theoretically.

Conflicts of interest

There are no conflicts to declare.

Acknowledgements

The National Natural Science Foundation of China (21773181, 21573172, and 21663024) has financially supported this work. X.Z. would like to acknowledge the financial support from the Nanotechnology Platform Program (Molecules and Materials Synthesis) of the Ministry of Education, Culture, Sports, Science, and Technology of Japan. K.Y. acknowledges the financial support from the ''Feitian Scholar Program of Gansu Province''.

Notes and references

1 K. S. Novoselov, A. K. Geim, S. V. Morozov, D. Jiang, Y. Zhang, S. V. Dubonos, I. V. Grigorieva and A. A. Firsov, Electric Field Effect in Atomically Thin Carbon Films, *Science*, 2004, **306**, 666–669.

2 D. C. Marcano, D. V. Kosynkin, J. M. Berlin, A. Sinitskii, Z. Z. Sun, A. Slesarev, L. B. Alemany, W. Lu and J. M. Tour, Improved synthesis of graphene oxide, *ACS Nano*, 2010, **4**, 4806–4814.

3 B. C. Brodie, XIII. On the atomic weight of graphite, *Philos. Trans. R. Soc.*, 1859, **149**, 249–259.

4 (*a*) J. W. Suk, R. D. Piner, J. An and R. S. Ruoff, Mechanical properties of monolayer graphene oxide, *ACS Nano*, 2010, **4**, 6557–6564; (*b*) J. E. Kim, T. H. Han, S. H. Lee, J. Y. Kim, C. W. Ahn, J. M. Yun and S. O. Kim, Graphene oxide liquid crystals, *Angew. Chem.*, 2011, **123**, 3099–3103.

5 (*a*) Q. Tang, Z. Zhou and Z. F. Chen, Graphene-related nanomaterials: tuning properties by functionalization, *Nanoscale*, 2013, **5**, 4541–4583; (*b*) J. T. Robinson, F. K. Perkins, E. S. Snow, Z. Q. Wei and P. E. Sheehan, Reduced graphene oxide molecular sensors, *Nano Lett.*, 2008, **8**, 3137–3140; (*c*) X. F. Gao, L. Wang, Y. Ohtsuka, D. E. Jiang, Y. L. Zhao, S. Nagase and Z. F. Chen, Oxidation unzipping of stable nanographenes into joint spin-rich fragments, *J. Am. Chem. Soc.*, 2009, **131**, 9663–9669; (*d*) K. P. Loh, Q. L. Bao, G. Eda and M. Chhowalla, Graphene oxide as a chemically tunable platform for optical applications, *Nat. Chem.*, 2010, **2**, 1015–1024; (*e*) G. Eda, G. Fanchini and M. Chhowalla, Large-area ultrathin films of reduced graphene oxide as a transparent and flexible electronic material, *Nat. Nanotechnol.*, 2008, **3**, 270–274.

6 N. Watanabe, T. Nakajima and H. Touhara, *Graphite Fluorides*, Elsevier, Amsterdam, 1988, pp. 23–89.

7 (*a*) M. H. F. Sluiter and Y. Kawazoe, Cluster expansion method for adsorption: Application to hydrogen chemisorption on graphene, *Phys. Rev. B: Condens. Matter Mater. Phys.*, 2003, **68**, 085410; (*b*) J. O. Sofo, A. S. Chaudhari and G. D. Barber, Graphane: A two-dimensional hydrocarbon, *Phys. Rev. B: Condens. Matter Mater. Phys.*, 2007, **75**, 153401.

8 D. C. Elias, R. R. Nair, T. M. G. Mohiuddin, S. V. Morozov, P. Blake, M. P. Halsall, A. C. Ferrari, D. W. Boukhvalov, M. I. Katsnelson, A. K. Geim and K. S. Novoselov, Control of graphene's properties by reversible hydrogenation: evidence for graphene, *Science*, 2009, **323**, 610–613.

9 M. Inagaki and F. Y. Kang, Graphene derivatives: graphane, fluorographene, graphene oxide, graphyne and graphdiyne, *J. Mater. Chem. A*, 2014, **2**, 13193–13206.

10 R. Balog, B. Jørgensen, L. Nilsson, M. Andersen, E. Rienks, M. Bianchi, M. Fanetti, E. Lægsgaard, A. Baraldi, S. Lizzit, Z. Sljivancanin, F. Besenbacher, B. Hammer, T. G. Pedersen, P. Hofmann and L. Hornekær, Bandgap opening in graphene induced by patterned hydrogen adsorption, *Nat. Mater.*, 2010, **9**, 315–319.

11 (*a*) J. T. Wang, C. F. Chen and Y. Kawazoe, Low-temperature phase transformation from graphite to sp3 orthorhombic carbon, *Phys. Rev. Lett.*, 2011, **106**, 075501; (*b*) Z. S. Zhao, B. Xu, X. F. Zhou, L. M. Wang, B. Wen, J. L. He, Z. Y. Liu, H. T. Wang and Y. J. Tian, Novel superhard carbon: C-centered orthorhombic C8, *Phys. Rev. Lett.*, 2011, **107**, 215502; (*c*) Z. P. Li, F. M. Gao and Z. M. Xu, Strength, hardness, and lattice vibrations of Z-carbon and W-carbon: first-principles calculations, *Phys. Rev. B: Condens. Matter Mater. Phys.*, 2012, **85**, 144115; (*d*) C. Y. Niu, X. Q. Wang and J. T. Wang, K6 carbon: A metallic carbon allotrope in sp3 bonding networks, *J. Chem. Phys.*, 2014, **140**, 054514; (*e*) J. Zhou, Q. Wang, Q. Sun and P. Jena, Intrinsic ferromagnetism in two-dimensional carbon structures: Triangular graphene nanoflakes linked by carbon chains, *Phys. Rev. B: Condens. Matter Mater. Phys.*, 2011, **84**, 081402(R); (*f*) M. Kan, J. Zhou, Y. W. Li and Q. Sun, Using carbon chains to mediate magnetic coupling in zigzag graphene nanoribbons, *Appl. Phys. Lett.*, 2012, **100**, 173106.

12 (*a*) G. X. Li, Y. L. Li, H. B. Liu, Y. B. Guo, Y. J. Li and D. B. Zhu, Architecture of graphdiyne nanoscale films, *Chem. Commun.*, 2010, **46**, 3256–3258; (*b*) X. W. Li, Q. Wang and P. Jena, Ferromagnetism in Two-Dimensional Carbon Chains Linked by 1,3,5-Benzenetriyl Units, *J. Phys. Chem. C*, 2011, **115**, 19621–19625.

13 R. Longuinhos, E. A. Moujaes, S. S. Alexandre and R. W. Nunes, Theoretical chemistry of α-graphyne: functionalization, symmetry breaking, and generation of Dirac-fermion mass, *Chem. Mater.*, 2014, **26**, 3701–3708.

14 G. Kresse and J. Furthmüller, Efficient Iterative Schemes for ab initio Total-Energy Calculations Using A Plane-Wave Basis Set, *Phys. Rev. B: Condens. Matter Mater. Phys.*, 1996, **54**, 11169–11186.

15 J. P. Perdew, K. Burke and M. Ernzerhof, Generalized Gradient Approximation Made Simple, *Phys. Rev. Lett.*, 1996, **77**, 3865–3868.

16 (*a*) P. Giannozzi, S. D. Gironcoli, P. Pavone and S. Baroni, Ab initio calculation of phonon dispersions in semiconductors, *Phys. Rev. B: Condens. Matter Mater. Phys.*, 1991, **43**, 7231–7242; (*b*) A. Togo and I. Tanaka, First principles phonon calculations in materials science, *Scr. Mater.*, 2015, **108**, 1–5.

17 (*a*) Z. B. Gao, X. Dong, N. B. Li and J. Ren, Novel two-dimensional silicon dioxide with in-plane negative Poisson's ratio, *Nano Lett.*, 2017, **17**, 772–777; (*b*) J. Heyd, G. E. Scuseria and M. Ernzerhof, Hybrid functionals based on a screened Coulomb potential, *J. Chem. Phys.*, 2003, **118**, 8207–8215.

18 V. Wang, N. Xu, J. C. Liu, G. Tang and W. T. Geng, VASPKIT: a user-friendly interface facilitating high-throughput computing and analysis using VASP code, arXiv preprint arXiv:1908.08269, 2019.

19 A. D. Becke, Density-functional thermochemistry. III. The role of exact exchange, *J. Chem. Phys.*, 1993, **98**, 5648–5652.

20 Z. B. Gao, M. Y. Li and J. S. Wang, Insight into Two-Dimensional Borophene: Five-Center Bond and Phonon-Mediated Superconductivity, *ACS Appl. Mater. Interfaces*, 2019, **11**, 47279–47288.

21 D. Y. Zubarev and A. I. Boldyrev, Developing paradigms of chemical bonding: adaptive natural density partitioning, *Phys. Chem. Chem. Phys.*, 2008, **10**, 5207–5217.

22 T. Lu and F. W. Chen, Multiwfn: a multifunctional wavefunction analyser, *J. Comput. Chem.*, 2012, **33**, 580–592.

23 M. J. Frisch, G. W. Trucks, H. B. Schlegel, G. E. Scuseria, M. A. Robb, J. R. Cheeseman, G. Scalmani, V. Barone, G. A. Petersson and H. Nakatsuji, *Gaussian 16, revision A.03*, Gaussian Inc., Wallingford CT, 2016.

24 (*a*) Y. Ohshima, S. Yamamoto, M. Nakata and K. Kuchitsu, Geometrical structure of allene studied by a joint analysis of electron-diffraction and spectroscopic data, *J. Phys. Chem.*, 1987, **91**, 4696–4700; (*b*) G. Trinquier and J. P. Malrieu, Nonclassical distortions at multiple bonds, *J. Am. Chem. Soc.*, 1987, **109**, 5303–5315.

25 O. Hod, Graphite and hexagonal boron-nitride have the same interlayer distance. Why?, *J. Chem. Theory Comput.*, 2012, **8**, 1360–1369.

26 X. X. Tian, X. Y. Xuan, M. Yu, Y. W. Mu, H. G. Lu, Z. H. Zhang and S. D. Li, Predicting two-dimensional semiconducting boron carbides, *Nanoscale*, 2019, **11**, 11099–11106.

27 H. Shin, S. Kang, J. Koo, H. Lee, J. Kim and Y. Kwon, Cohesion energetics of carbon allotropes: Quantum Monte Carlo study, *J. Chem. Phys.*, 2014, **140**, 114702.

28 (*a*) S. H. Zhang, J. Zhou, Q. Wang, X. S. Chen, Y. Kawazoe and P. Jena, Penta-graphene: A new carbon allotrope, *Proc. Natl. Acad. Sci. U. S. A.*, 2015, **112**, 2372–2377; (*b*) Y. Ding and Y. L. Wang, Density functional theory study of the silicene-like SiX and XSi3 (X = B, C, N, Al, P) honeycomb lattices: the various buckled structures and versatile electronic properties, *J. Phys. Chem. C*, 2013, **117**, 18266–18278; (*c*) M. Y. Li, K. Yuan, Y. X. Zhao, Z. B. Gao and X. Zhao, A Novel Hyperbolic Two-Dimensional Carbon Material with an In-Plane Negative Poisson's Ratio Behavior and Low-Gap Semiconductor Characteristics, *ACS Omega*, 2020, **5**, 15783–15790; (*d*) T. S. Zhao, S. H. Zhang, Y. G. Guo and Q. Wang, TiC2: a new two-dimensional sheet beyond MXenes, *Nanoscale*, 2016, **8**, 233–242.

29 (*a*) Z. B. Gao, Z. F. Zhang, G. Liu and J. S. Wang, Ultra-low lattice thermal conductivity of monolayer penta-silicene and penta-germanene, *Phys. Chem. Chem. Phys.*, 2019, **21**, 26033–26040; (*b*) X. C. Shang and S. L. Roderic, Stability of elastic material with negative stiffness and negative Poisson's ratio, *Phys. Status Solidi*, 2007, **244**, 1008–1026.

30 (*a*) H. Sugimoto, M. Fujii and K. Imakita, Size-controlled growth of cubic boron phosphide nanocrystals, *RSC Adv.*, 2015, **5**, 8427–8431; (*b*) J. A. Andrade-Arvizu, M. F. García-Sánchez, M. Courel-Piedrahita, J. Santoyo-Morales, D. Jiménez-Olarte, M. Albor-Aguilera and O. Vigil-Galán, Pressure induced directional transformations on close spaced vapor transport deposited SnS thin films, *Mater. Des.*, 2016, **110**, 878–887; (*c*) S. Liu, R. He, L. J. Xue, J. H. Li, B. Liu and J. H. Edgar, Single crystal growth of millimeter-sized monoisotopic hexagonal boron nitride, *Chem. Mater.*, 2018, **30**, 6222–6225; (*d*) T. Sudare, C. Mori, F. Hayashi and K. Teshima, Fabrication of fluorapatite nanocrystal-activated carbon composite by the atmospheric pressure plasma-assisted flux method, *Cryst. Growth Des.*, 2018, **18**, 5763–5769; (*e*) L. A. Walsh and C. L. Hinkle, van der Waals epitaxy: 2D materials and topological insulators, *Appl. Mater. Today*, 2017, **9**, 504–515.

31 (*a*) I. A. Popov and A. I. Boldyrev, Chemical bonding in coronene, isocoronene, and circumcoronene, *Eur. J. Org. Chem.*, 2012, 3485–3491; (*b*) I. A. Popov, Y. F. Li, Z. F. Chen and A. I. Boldyrev, ''Benzation'' of graphene upon addition of monovalent chemical species, *Phys. Chem. Chem. Phys.*, 2013, **15**, 6842–6848; (*c*) I. A. Popov, K. V. Bozhenko and A. I. Boldyrev, Is graphene aromatic?, *Nano Res.*, 2012, **5**, 117–123.

32 (*a*) Z. N. Ma, B. Wang, L. K. Ou, Y. Zhang, X. Zhang and Z. Zhou, Structure and properties of phosphorene-like IV-VI 2D materials, *Nanotechnology*, 2016, **27**, 415203; (*b*) Y. H. Liu, B. Yang, M. Y. Zhang, B. Xia, C. Chen,

X. P. Liu, J. Zhong, Z. W. Xiao and J. Tang, Bournonite CuPbSbS3: An electronically-3D, defect-tolerant, and solution-processable semiconductor for efficient solar cells, *Nano Energy*, 2020, **71**, 104574; (*c*) S. Dutta and S. K. Pati, Novel properties of graphene nanoribbons: a review, *J. Mater. Chem.*, 2010, **20**, 8207–8223.

33 (*a*) H. Liu, Y. Liu and D. Zhu, Chemical doping of graphene, *J. Mater. Chem.*, 2011, **21**, 3335–3345; (*b*) L. Yan, Y. B. Zheng, F. Zhao, S. J. Li, X. F. Gao, B. Q. Xu, P. S. Weiss and Y. L. Zhao, Chemistry and physics of a single atomic layer: strategies and challenges for functionalization of graphene and graphene-based materials, *Chem. Soc. Rev.*, 2012, **41**, 97–114.

34 M. C. Sun, Y. Q. Sui, K. Gao, C. Tan, L. Dai, G. P. Zhou, Y. J. Zhang and L. Wang, Theoretical analysis of thermal and mechanical properties of Eu2Hf2O7 and Gd2Hf2O7 pyrochlores, *J. Ceram. Soc. Jpn.*, 2019, **127**, 722–727.

35 (*a*) L. Z. Kou, C. F. Chen and S. C. Smith, Phosphorene: fabrication, properties, and applications, *J. Phys. Chem. Lett.*, 2015, **6**, 2794–2805; (*b*) J. W. Jiang and H. S. Park, Negative Poisson's ratio in single-layer black phosphorus, *Nat. Commun.*, 2014, **5**, 4727.

36 O. L. Anderson, A simplified method for calculating the Debye temperature from elastic constants, *J. Phys. Chem. Solids*, 1963, **24**, 909–917.

37 F. R. L. Schoening and L. A. Vermeulen, X-ray measurement of the Debye temperature for diamond at low temperatures, *Solid State Commun.*, 1969, **7**, 15–18.

38 D. R. Chipman, Temperature Dependence of the Debye Temperatures of Aluminum, Lead, and Beta Brass by an X-Ray Method, *J. Appl. Phys.*, 1960, **31**, 2012–2015.

39 (*a*) A. Jalil, Z. W. Zhuo, Z. T. Sun, F. Wu, C. Wang and X. J. Wu, A phosphorene-like InP3 monolayer: structure, stability, and catalytic properties toward the hydrogen evolution reaction, *J. Mater. Chem. A*, 2020, **8**, 1307–1314; (*b*) H. H. Wu, H. Huang, J. Zhong, S. Yu, Q. B. Zhang and X. C. Zeng, Monolayer triphosphates MP3 (M= Sn, Ge) with excellent basal catalytic activity for hydrogen evolution reaction, *Nanoscale*, 2019, **11**, 12210–12219; (*c*) S. S. Chou, N. Sai, P. Lu, E. N. Coker, S. Liu, K. Artyushkova, T. S. Luk, B. Kaehr and C. J. Brinker, Atomically thin resonant tunnel diodes built from synthetic van der Waals heterostructures, *Nat. Commun.*, 2015, **6**, 8311; (*d*) X. T. Li, Y. Y. Wan and X. J. Wu, First-principles study of ultrathin molybdenum sulfides nanowires: Electronic and catalytic hydrogen evolution properties, *Chin. J. Chem. Phys.*, 2019, **32**, 267–272; (*e*) J. Q. Zhu, Z. C. Wang, H. J. Dai, Q. Q. Wang, R. Yang, H. Yu, M. Z. Liao, J. Zhang, W. Chen, Z. Wei, N. Li, L. J. Du, D. X. Shi, W. L. Wang, L. X. Zhang, Y. Jiang and G. Y. Zhang, Boundary activated hydrogen evolution reaction on monolayer MoS2, *Nat. Commun.*, 2019, **10**, 1348; (*f*) D. Voiry, H. Yamaguchi, J. W. Li, R. Silva, D. C. B. Alves, T. Fujita, M. W. Chen, T. Asefa, V. B. Shenoy, G. Eda and M. Chhowalla, Enhanced catalytic activity in strained chemically exfoliated WS2 nanosheets for hydrogen evolution, *Nat. Mater.*, 2013, **12**, 850–855; (*g*) M. Jahan, Z. L. Liu and K. P. Loh, A Graphene oxide and copper-centered metal organic framework composite as a tri-functional catalyst for HER, OER, and ORR, *Adv. Funct. Mater.*, 2013, **23**, 5363–5372; (*h*) Y. Ito, W. T. Cong, T. Fujita, Z. Tang and M. W. Chen, High catalytic activity of nitrogen and sulfur co-doped nanoporous graphene in the hydrogen evolution reaction, *Angew. Chem.*, 2015, **54**, 2131–2136.

40 A. G. M. Ferrari, D. A. C. Brownson and C. E. Banks, Investigating the integrity of Graphene towards the electrochemical Hydrogen evolution Reaction (HER), *Sci. Rep.*, 2019, **9**, 1–10.

